# Sakata model of hadrons revisited. II. Nuclei and scattering

Eugene V. Stefanovich
*2255 Showers drive, Apt. 153, Mountain View, CA 94040, USA*
*eugene_stefanovich@usa.net*

July 6, 2015

**Abstract**

This article continues our previous study in arXiv:1010.0458. Sakaton interactions potentials are re-optimized. Masses of mesons, baryons, light nuclei and hypernuclei are obtained in a good agreement with experiment. Scattering cross sections ($pp$, $p\overline{p}$, $np$, and $\Lambda p$) appear overestimated, especially at high energies. This suggests that using interaction potentials that are nonsingular at $r = 0$ would lead to a better agreement with experiments. In general, our results indicate that Sakata model may be a promising replacement for the quark model of hadrons.

## 1 Introduction

Quark model is universally accepted as the foundation of the modern theory of strong nuclear interactions and the entire Standard Model. In spite of its successes, the idea of quarks is vulnerable to criticism as well. For example, the postulated quarks and gluons cannot be directly observed, even in principle. These particles are assumed to possess very unusual properties: fractional electric charges and non-observable color. The mechanism of quark confinement inside mesons and baryons has not been understood yet. Quantum chromodynamics is a non-Abelian gauge quantum field theory. Calculations of even simplest bound states or low-energy scattering processes are notoriously difficult in this approach.

So, one is tempted to ask provocative questions: is the nature of strong interactions bound to be so complicated? are there alternative ways to think about physics of hadrons? One such alternative idea was proposed by S. Sakata in 1956 [1], i.e., long before the advent of the quark model. The beauty of the Sakata model was that

the number of arbitrary assumptions was reduced to a minimum there. Elementary constituents (sakatons) were chosen to be the familiar proton ($p$), neutron ($n$), and Lambda-hyperon ($\Lambda$).[1] If one assumes[2] that sakaton-antisakaton interaction potentials are strongly attractive, but sakaton-sakaton and sakaton-antisakaton potentials are equally repulsive, then one can describe the mass spectrum of hadrons in a remarkable agreement with observations even without full quantum mechanical calculations [3, 4]. For example, in the Sakata model the pion is identified with a sakaton-antisakaton bound state $\pi^- = n\overline{p}$, so that its mass is composed from the masses of constituents $m(n) = m(\overline{p}) = 940\ MeV/c^2$ and the energy of their attraction. The latter can be estimated from the known value $m(\pi^-) = 140\ MeV/c^2$ as $V(n, \overline{p}) \approx -1740\ MeV$, so that

$$m(\pi^-) = m(n\overline{p}) = m(n) + m(p) + V(n, \overline{p})/c^2 = 940 + 940 - 1740 = 140\ MeV/c^2$$

Assuming that $n$ and $p$ have equal interaction strengths with $\Lambda$,[3] one can immediately evaluate the mass of the $\Sigma^-$ baryon[4]

$$\begin{aligned} m(\Sigma^-) &= m(\Lambda n\overline{p}) = m(\Lambda) + m(n) + m(p) + V(\Lambda, n)/c^2 + V(\Lambda, \overline{p})/c^2 + V(n, \overline{p})/c^2 \\ &= 1116 + 940 + 940 - 1740 = 1256\ MeV/c^2 \end{aligned}$$

Of course, one cannot expect this simplistic approach to work in all cases. For example, in addition to explaining the stability of the famous $\Omega^- = \Lambda\Lambda\Lambda\overline{pn}$ particle, the Matumoto mass formula [3, 4] incorrectly predicted the same masses and stabilities for two other members of the triplet $\Omega^{--} = \Lambda\Lambda\Lambda\overline{pp}$ and $\Omega^0 = \Lambda\Lambda\Lambda\overline{nn}$, which have not been observed.

In our previous publication [2] we tried to go beyond the simple mass formula. We designed a set of inter-sakaton potentials and calculated masses of multisakaton bound states by numerical solution of corresponding Schrödinger equations. A good agreement was obtained with the mass spectrum and stabilities of known mesons and baryons. However, there were also two areas where our previous results appeared inadequate:

1. When attempting to model particle collisions, we found that scattering cross sections of hadrons were overestimated by several orders of magnitude.

[1] In this work we consider only systems possessing up, down, and strange flavors. By adding the fourth elementary hadron $\Lambda_c^+$, one can extend the Sakata model to charmed particles as well [2].

[2] in analogy with electrostatic interactions between charges

[3] e.g., $V(\Lambda, n) = -V(\Lambda, \overline{p})$

[4] the experimental value is $m(\Sigma^-) = 1189\ MeV/c^2$

2. Our $pn$, $pp$ and $nn$ potentials were completely repulsive, so they could not explain the binding of protons and neutrons in nuclei.

In this work we decided to recalibrate sakaton interaction potentials for better description of these two important aspects.

# 2 Theory and computational details

## 2.1 Model Hamiltonian

In our opinion, it should be possible to build theory of strong interactions based on the idea of point particles interacting by instantaneous forces. This belief is supported by the success of the "dressed particle" approach to quantum electrodynamics [5, 6], where various electromagnetic phenomena were explained without invoking (quantum or classical) fields.

Thus we describe an interacting $\mathcal{N}$-sakaton system by the approximate non-relativistic Hamiltonian

$$H = \sum_{i=1}^{\mathcal{N}} m_i c^2 + \sum_{i=1}^{\mathcal{N}} \frac{p_i^2}{2m_i} + \sum_{i<j}^{\mathcal{N}} V_{ij}(r_{ij}) \tag{1}$$

where $\mathbf{p}_i, r_{ij} \equiv |\mathbf{r}_i - \mathbf{r}_j|$ are momenta of the sakatons and their relative distances, respectively. Masses $m_i$ of sakatons are shown in Table 1.

Table 1: Model properties of sakatons.

| sakaton symbol | Mass MeV/$c^2$ | Electric charge | Strangeness | Spin |
|---|---|---|---|---|
| $n$ | 940 | 0 | 0 | 1/2 |
| $p$ | 940 | 1 | 0 | 1/2 |
| $\Lambda$ | 1116 | 0 | -1 | 1/2 |

Interaction potentials are modeled as superpositions of three Yukawa functions

$$V_{ij}(r) = A_{ij} z_i z_j \frac{e^{-\alpha_{ij} r}}{r} + B_{ij} \frac{e^{-\beta_{ij} r}}{r} + C_{ij} z_i z_j \frac{e^{-\gamma_{ij} r}}{r} \tag{2}$$

where $z_i = +1$ for sakatons and $z_i = -1$ for antisakatons. Optimized parameters of these potentials are collected in Table 2. Interaction (2) consists of three parts: the first term is of the Matumoto type. It corresponds to attraction in sakaton-antisakaton

pairs ($z_i z_j = -1$) and equal repulsion in sakaton-sakaton and antisakaton-antisakaton pairs ($z_i z_j = 1$). Our preliminary tests indicated that this interaction alone was inadequate as it systematically overestimated binding and thus predicted stability of many nonexistent species. Some extra repulsion is added by the second term. The third term is designed to represent the (relatively) long-range (r$\approx$ 1 $fm$) nucleon-nucleon attraction in nuclei [2].

Table 2: Parameters of sakaton-sakaton interaction potentials (2) optimized in this work.

| | $A$ MeV·fm | $\alpha$ fm$^{-1}$ | $B$ MeV·fm | $\beta$ fm$^{-1}$ | $C$ MeV·fm | $\gamma$ fm$^{-1}$ |
|---|---|---|---|---|---|---|
| $p-p$ | 2137 | 8.2 | 1119 | 10.04 | -12 | 0.125 |
| $n-n$ | 2137 | 8.2 | 1119 | 10.04 | -12 | 0.125 |
| $p-n$ | 1610 | 7.02 | 886.6 | 14.55 | -18.6 | 0.106 |
| $p-\Lambda$ | 1334 | 7.245 | 386.8 | 10.726 | -21 | 0.25 |
| $n-\Lambda$ | 1334 | 7.245 | 386.8 | 10.726 | -21 | 0.25 |
| $\Lambda-\Lambda$ | 709 | 9.13 | 500 | 11.15 | -22 | 0.30 |

As an example, in Fig. 1 we show the proton-proton interaction potential (thick full line) whose general shape is familiar from textbooks in nuclear physics. The proton-neutron potential (thin full line) has a similar shape, but the attractive well at $r \approx 1\ fm$ is somewhat deeper, so that a bound state of the deuteron ($pn$) can be supported (see Table 5). The proton-antiproton ($p\overline{p}$) interaction (broken line) is almost a mirror image of the $pp$ potential. Other sakaton-antisakaton potentials have similar shapes. Their strong attraction at $r < 0.5\ fm$ is responsible for holding mesons and baryons together.

Note that in our model $p$ and $n$ sakatons have equal masses and the same interaction parameters. This implies that all calculated properties (e.g., masses and scattering cross-sections) of multisakaton systems are invariant with respect to simultaneous sakaton replacements $p \leftrightarrow n$.

## 2.2 Bound state calculations

Bound state energies of multisakaton systems were calculated using the stochastic variational method of Varga and Suzuki [7, 8, 9]. Only states with the lowest total spin ($s = 0$ for bosons and $s = 1/2$ for fermions) and zero orbital momentum were considered here. The basis set size depended on the number of sakatons in the system. For mixed sakaton-antisakaton species with particle numbers $\mathcal{N} = 2, 3, 4, 5$ the basis size was $K = 50, 220, 250$ and 800, respectively. For sakaton-only species (i.e., nuclei) the basis size $K = 50$ was independent on the number of particles. For other computational

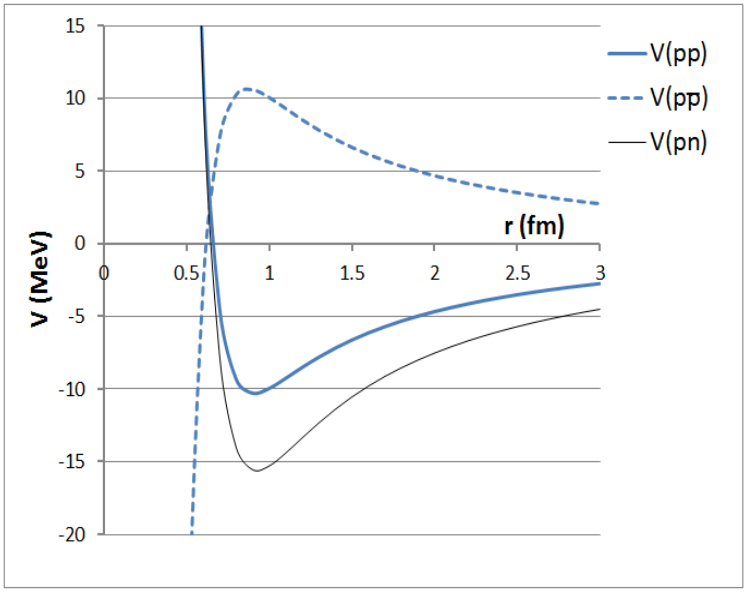


Figure 1: Interaction potentials: proton-proton (thick full line), proton-neutron (thin full line), and proton-antiproton (broken line).

parameters [7] we used values $M_0 = 10, K_0 = 50, b_{min} = 10^{-6}$, and $b_{max} = 10$ adjusted for optimal balance between accuracy and the speed of convergence.

## 2.3 Scattering calculations

Scattering calculations were performed in the first Born approximation [10, 11]. For scattering of two particles with momenta $\mathbf{p}_1 = -\mathbf{p}_2 \equiv \mathbf{p}_{c.m}$ in the center-of-mass frame the differential cross section was calculated as[5]

$$\frac{d\sigma}{d\Omega} = \frac{(2\pi)^4\hbar^2}{c^4(\frac{1}{E_1(p_{c.m.})} + \frac{1}{E_2(p_{c.m.})})^2}|T_B(\mathbf{k})|^2 \tag{3}$$

where $E_i(p) \equiv \sqrt{m_i^2c^4 + p^2c^2}$ are energies of the colliding particles, $\mathbf{k} \equiv \mathbf{p}_1' - \mathbf{p}_1$ is the transferred momentum and the matrix element $T_B$ is the Fourier transform of the interaction potential

$$T_B(\mathbf{k}) = \frac{1}{(2\pi\hbar)^3}\int d\mathbf{r}e^{\frac{i}{\hbar}\mathbf{kr}}V(\mathbf{r}) \tag{4}$$

[5] see equation (3.149) in [11]

For comparison with experiments it was convenient to rewrite $d\sigma/d\Omega$ as a function of invariant Mandelstam variables $s \equiv (\tilde{p}_1 + \tilde{p}_2)^2$ and $t \equiv (\tilde{p}_1 - \tilde{p}_1')^2$, which have simple meanings in the center of mass frame

$$\begin{aligned} s &= (E_1(p_{c.m.}) + E_2(p_{c.m.}))^2 \\ t &= -c^2k^2 = 2c^2p_{c.m.}(\cos\theta - 1) \end{aligned} \tag{5}$$

where $\theta$ is the scattering angle (between vectors $\mathbf{p}_1'$ and $\mathbf{p}_1$). Taking into account (5) and $d\Omega = 2\pi d(\cos\theta)$, we obtain (in the case of equal masses $m_1 = m_2 = m$)

$$\frac{d\sigma}{dt} = \frac{d\sigma}{d\Omega} \cdot \frac{2\pi}{dt/d(\cos\theta)} = \frac{d\sigma}{d\Omega} \cdot \frac{\pi}{c^2p_{c.m.}^2} = \frac{d\sigma}{d\Omega} \cdot \frac{4\pi}{s - 4m^2c^2} \tag{6}$$

The total elastic cross section was calculated by integrating the differential cross section (3) on angles

$$\sigma_{elastic}(p_{c.m.}) = 2\pi \int_0^\pi \sin\theta d\theta \frac{d\sigma}{d\Omega} \tag{7}$$

For easier comparison with experiments we switched to the laboratory reference frame[6] and expressed $\sigma_{elastic}$ as a function of the "lab frame" momentum of the incoming particle [7]

$$p_{lab} = p_{c.m.}\sqrt{s}/(m_2c)$$

So, in the case of equal masses, the lab frame cross section was obtained by replacing $p_{c.m.}^2 \to (mc\sqrt{m^2c^2 + p_{c.m.}^2} - m^2c^2)/2$ in formula (7).

Our calculations for both binding energies and cross sections were, of course, approximate as they ignored important relativistic and high order perturbation corrections. Nevertheless, we believe that most significant physical effects were captured by this model, and the results could be trusted within order of magnitude.

# 3 Results

## 3.1 Bound states of sakatons

As we discussed above, according to the Sakata model, all mesons and baryons, except $p$, $n$, and $\Lambda^0$, are in fact composite systems built from the above elementary sakatons

[6] where the "target" particle 2 is at rest

[7] see eq. (46.36) in [12]

and antisakatons. Atomic nuclei can be also regarded as multisakaton bound states. So, the first challenge for our model was to explain the stability[8] pattern of simplest compound systems listed in Table 3.

Table 3: Summary table of compound hadrons considered in this work. Notation: $\sigma = (p, n, \Lambda)$ stands for all sakatons; $\nu = (p, n)$ stands for nucleons.

| Sakaton composition | Particle type | Comments | see Table |
|---|---|---|---|
| $\sigma\overline{\sigma}$ | simple mesons | all stable except $\Lambda\overline{\Lambda}$ | 4 |
| $\sigma\sigma\overline{\sigma\sigma}$ | tetrasakaton mesons | all unstable | |
| $\sigma\sigma\overline{\sigma}$ | simple baryons | all unstable except $\Sigma$ and $\Xi$ | 4 |
| $\sigma\sigma\sigma\overline{\sigma\sigma}$ | pentasakaton baryons | all unstable except $\Omega^-$ | 4 |
| $\nu\nu\ldots\nu$ | nuclei | | 5 |
| $\nu\Lambda, \Lambda\Lambda, \nu\nu\Lambda, \nu\Lambda\Lambda$ | hypernuclei | | 6 |

As shown in Table 4, masses of stable mesons and baryons are reproduced reasonably well in our model. In agreement with experiment, no stable tetrasakaton mesons were found and the only stable pentasakaton baryon is the $\Omega^- = \Lambda\Lambda\Lambda\overline{pn}$ particle.

Table 4: Stable compound mesons and baryons

| Stable particle | Sakaton composition | Calc. mass $MeV/c^2$ | Exp. mass $MeV/c^2$ | Calc. Binding energy (MeV) | Exp. Binding energy (MeV) |
|---|---|---|---|---|---|
| $\pi^0$ | $(p\overline{p}, n\overline{n})$ | 323.99 | **135** | $1556.01(\rightarrow p+\overline{p})$ | $\mathbf{1733}(\rightarrow p+\overline{n})$ |
| $\pi^+$ | $p\overline{n}$ | 338.21 | **140** | $1541.79(\rightarrow p+\overline{n})$ | $\mathbf{1734}(\rightarrow p+\overline{n})$ |
| $\pi^-$ | $n\overline{p}$ | 338.21 | **140** | $1541.79(\rightarrow n+\overline{p})$ | $\mathbf{1734}(\rightarrow n+\overline{p})$ |
| $K^0$ | $\Lambda\overline{n}$ | 499.46 | **498** | $1556.54(\rightarrow \Lambda+\overline{n})$ | $\mathbf{1558}(\rightarrow \Lambda+\overline{n})$ |
| $K^-$ | $\Lambda\overline{p}$ | 499.46 | **494** | $1556.54(\rightarrow \Lambda+\overline{p})$ | $\mathbf{1556}(\rightarrow \Lambda+\overline{p})$ |
| $\Sigma^0$ | $(\Lambda p\overline{p}, \Lambda n\overline{n})$ | 1428.13 | **1193** | $11.33(\rightarrow p+\Lambda\overline{p})$ | $\mathbf{58}(\rightarrow \Lambda+p\overline{p})$ |
| $\Sigma^+$ | $\Lambda p\overline{n}$ | 1400.47 | **1189** | $38.99(\rightarrow p+\Lambda\overline{n})$ | $\mathbf{67}(\rightarrow \Lambda+p\overline{n})$ |
| $\Sigma^-$ | $\Lambda n\overline{p}$ | 1400.47 | **1189** | $38.99(\rightarrow n+\Lambda\overline{p})$ | $\mathbf{67}(\rightarrow \Lambda+n\overline{p})$ |
| $\Xi^0$ | $\Lambda\Lambda\overline{n}$ | 1231.32 | **1315** | $388.14\ (\rightarrow \Lambda+\Lambda\overline{n})$ | $\mathbf{299}(\rightarrow \Lambda+\Lambda\overline{n})$ |
| $\Xi^-$ | $\Lambda\Lambda\overline{p}$ | 1231.32 | **1322** | $388.14\ (\rightarrow \Lambda+\Lambda\overline{p})$ | $\mathbf{288}\ (\rightarrow \Lambda+\Lambda\overline{p})$ |
| $\Omega^-$ | $\Lambda\Lambda\Lambda\overline{pn}$ | 1720.95 | **1672** | $9.83(\rightarrow \Lambda\Lambda\overline{n}+\Lambda\overline{p})$ | $\mathbf{137}(\rightarrow \Lambda\Lambda\overline{n}+\Lambda\overline{p})$ |

As we mentioned in subsection 2.1, our potentials (2) can describe nucleon-nucleon binding in atomic nuclei. Indeed, results presented in Table 5 demonstrate that the

[8]We are interested only in stability with respect to strong interactions. Particles experiencing weak and/or electromagnetic decays are regarded as stable here.

nuclear stability pattern is represented fairly well up to the $^{6}$Be nucleus. However, the nuclear binding energies are systematically underestimated, which indicates that *pp*, *pn*, and *nn* attractions are probably too low in our model.[9]

Table 5: Binding energies (with respect to complete dissociation) of nuclei.

| Sakaton composition | Nuclear symbol | Exp. binding energy (MeV) [13] | Calc. binding energy (MeV) |
|---|---|---|---|
| *pp* | | 0 | 0 |
| *pn* | $^{2}$H | **2.22** | 0.44 |
| *nn* | | 0 | 0 |
| *ppp* | | 0 | diverged |
| *ppn* | $^{3}$He | **7.72** | 1.75 |
| *pnn* | $^{3}$H | **8.48** | 1.75 |
| *nnn* | | 0 | diverged |
| *pppp* | | 0 | 0 |
| *pppn* | $^{4}$Li | **4.62** | 1.10 |
| *ppnn* | $^{4}$He | **28.30** | 1.08 |
| *pnnn* | $^{4}$H | **5.50** | 1.10 |
| *nnnn* | | 0 | 0 |
| *ppppp* | | 0 | diverged |
| *ppppn* | | 0 | 0 |
| *pppnn* | $^{5}$Li | **26.33** | 5.23 |
| *ppnnn* | $^{5}$He | **27.41** | 5.23 |
| *pnnnn* | $^{5}$H | **1.08** | 0 |
| *nnnnn* | | 0 | diverged |
| *pppppp* | | 0 | 0 |
| *pppppn* | | 0 | 0 |
| *pppnn* | $^{6}$Be | **26.92** | 9.10 |
| *pppnnn* | $^{6}$Li | **31.99** | 10.84 |
| *ppnnnn* | $^{6}$He | **29.27** | 9.10 |
| *pnnnnn* | $^{6}$H | **5.78** | 0 |
| *nnnnnn* | | 0 | 0 |

Similar results are presented in Table 6 for hypernuclei, i.e., nuclei where one or more neutrons are replaced by $\Lambda^0$ particles. Our model correctly predicts the absence of $p\Lambda$, $n\Lambda$, and $\Lambda\Lambda$ bound states. However, the binding energy of the ${}^{3}_{\Lambda}H$ species is underestimated, and the model predicts positive binding of several non-existent

[9]For some species shown in the Table, our calculations did not converge, probably due to numerical instability of the FORTRAN code.

hypernuclei. This indicates that our optimized interaction parameters in Table 2 are not well balanced.

Table 6: Binding energies (with respect to complete dissociation) of hypernuclei.

| Sakaton composition | Nuclear symbol | Exp. Binding energy (MeV) [14] | Calc. Binding energy (MeV) |
|---|---|---|---|
| $p\Lambda$ | | 0 | 0 |
| $n\Lambda$ | | 0 | 0 |
| $\Lambda\Lambda$ | | 0 | 0 |
| $pp\Lambda$ | | 0 | 0.52 |
| $pn\Lambda$ | ${}^{3}_{\Lambda}H$ | **2.35** | 1.30 |
| $nn\Lambda$ | | 0 | 0.52 |
| $p\Lambda\Lambda$ | | 0 | 0.72 |
| $n\Lambda\Lambda$ | | 0 | 0.72 |
| $\Lambda\Lambda\Lambda$ | | 0 | diverged |

### 3.2 Elastic scattering

Total elastic cross sections for $pp$, $p\overline{p}$, $np$, and $\Lambda p$ collisions are shown in Figs. 2, 3, 4, and 5, respectively. Note that agreement with experiments has improved significantly since our earlier attempts [2], but even the latest calculated $\sigma_{elastic}$ are overestimated by several orders of magnitude, especially at high collision energies.

## 4 Discussion and conclusions

In spite of some deviations, meson, baryon, and nuclear stability patterns are reproduced quite well in our studies. The most remarkable is the fact that the model predicts positive binding energies for all existing mesons and baryons, while dozens of exotic $\sigma\sigma\overline{\sigma}\overline{\sigma}$ and $\sigma\sigma\sigma\overline{\sigma}\overline{\sigma}$ species turn out to be unstable in calculations. This is a strong indication that sakaton potentials optimized here as well as the Sakata model itself do capture some important aspects of the physics of hadrons.

The most troublesome are calculated elastic scattering cross sections that deviate significantly from experiments, as shown in Figs. 2 - 5. To understand this behavior, we can turn to differential cross sections for $pp$ collisions at $\sqrt{s} = 19.4\ GeV$ shown in Fig. 6. According to (3), (4), and (5), the differential cross section $d\sigma/dt$ as a function of the transferred momentum $\sqrt{-t}/c$ is proportional to the Fourier transform (4) of $V(r)$. Thus all features on the graph 6 should be traceable to their origins in the shape of the position-space interaction potential. For example, the characteristic dip on the

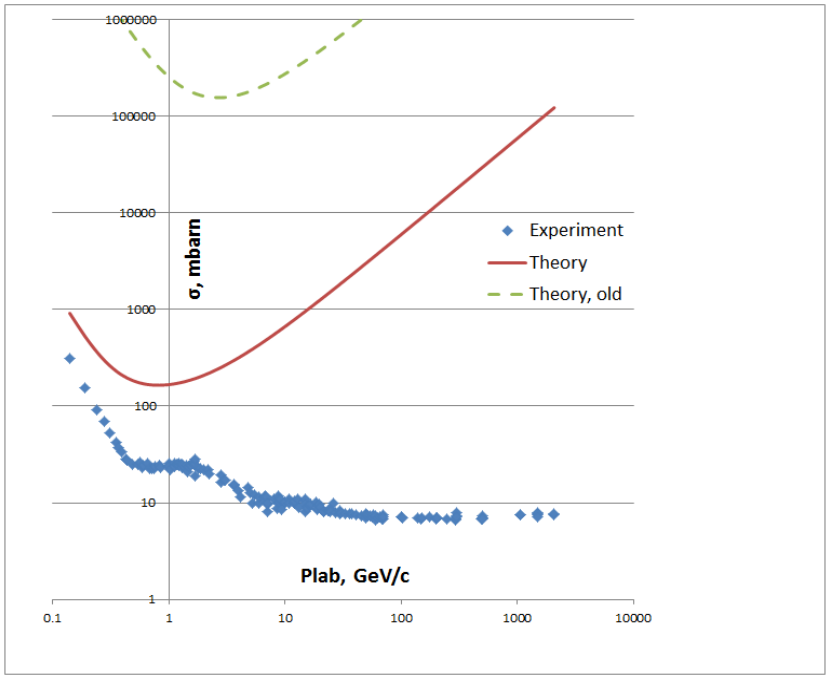


Figure 2: Total elastic cross section for $pp$ collisions. Experimental data from [12]. "Old" theory from [2].

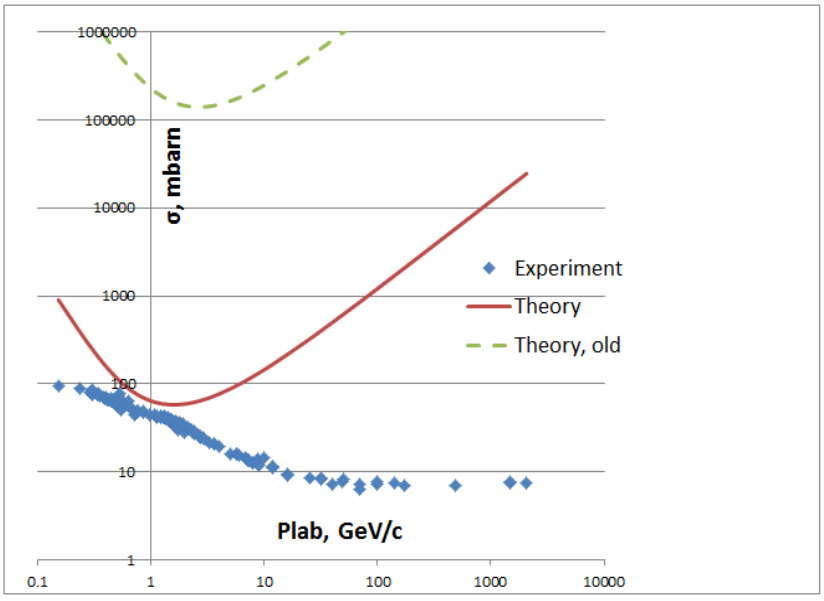


Figure 3: Total elastic cross section for $p\overline{p}$ collisions. Experimental data from [12]. "Old" theory from [2].

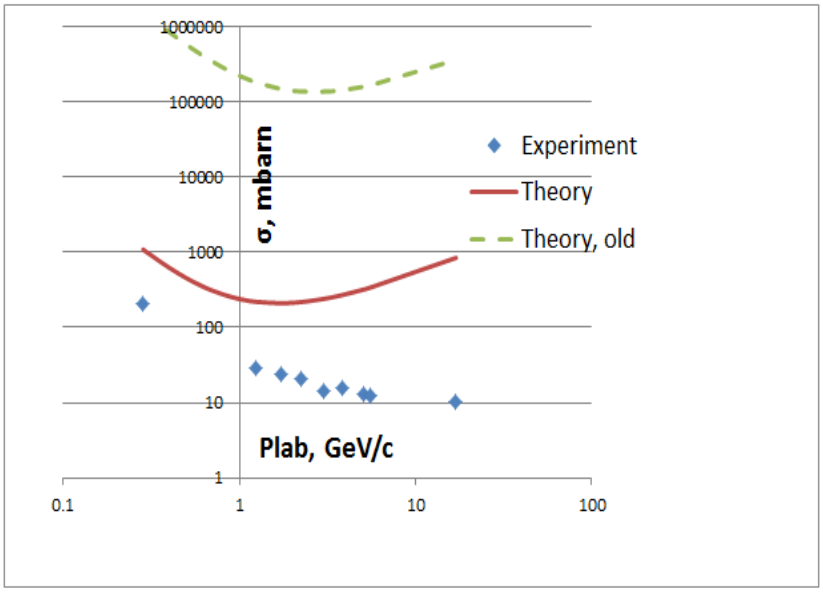


Figure 4: Total elastic cross section for $np$ collisions. Experimental data from [12]. "Old" theory from [2].

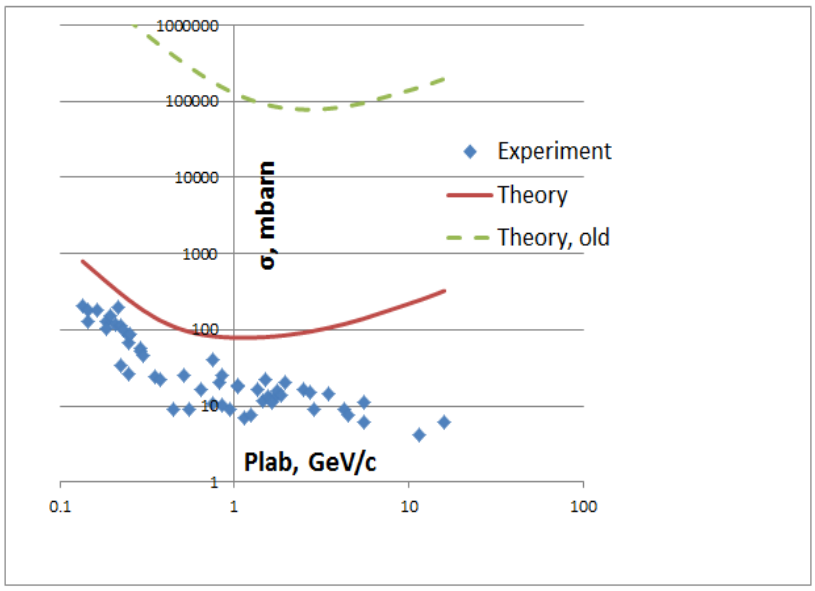


Figure 5: Total elastic cross section for $\Lambda p$ collisions. Experimental data from [12]. "Old" theory from [2].

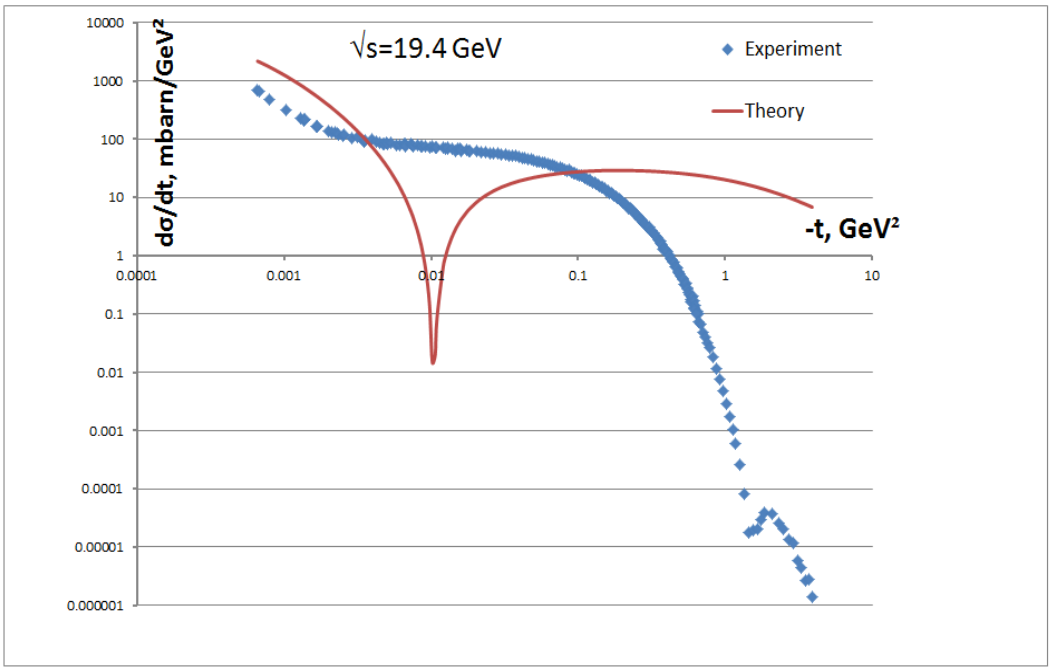


Figure 6: Differential cross section $d\sigma/dt$ for elastic $pp$ collisions at $\sqrt{s} = 19.4$ GeV. Experimental data from [15].

theoretical $d\sigma/dt(t)$ curve at $t \approx -0.1\ GeV^2$ has its explanation in the fact that the $pp$ potential (see Fig. 1) changes its sign around $r \approx 0.65\ fm$ from repulsive to attractive. It is likely that a similar dip on the experimental curve has the same nature, though it is shifted to higher momenta ($t \approx -1.5\ GeV^2$) with respect to our result.

The largest discrepancies are at high transferred momenta. Experimental values drop sharply at $t < -0.1\ GeV^2$, but our calculated cross section remains almost constant there, which is the reason for overestimation of the total elastic cross section in our model. This slow asymptotic decline of the Fourier transform ($d\sigma/dt$) reflects singular character of the position-space interaction potential (2) at $r = 0$. So, it is reasonable to assume that a better agreement with scattering data can be achieved if, instead of Yukawa-type potentials (2), we choose non-singular sakaton-sakaton interactions, like $V(r) \propto e^{-\alpha r}$ or $V(r) \propto e^{-\alpha r^2}$. Parameter optimization for such interactions is currently underway.

# References

[1] S. Sakata, "On a composite model for the new particles," *Prog. Theor. Phys.*, vol. **16**, p. 686, 1956.

[2] E. V. Stefanovich, "Sakata model of hadrons revisited," 2010. arXiv:1010.04058v1.

[3] K. Matumoto, "Some consequences of the compound hypothesis for elementary particles," *Prog. Theor. Phys.*, vol. **16**, p. 583, 1956.

[4] K. Matumoto, S. Sawada, Y. Sumi, and M. Yonezawa, "Mass formula in the Sakata model," *Prog. Theor. Phys. Suppl.*, vol. **19**, p. 66, 1961.

[5] E. V. Stefanovich, "Relativistic quantum dynamics," 2005. arXiv:physics/0504062v17.

[6] A. V. Shebeko, "Clothed particles in mesodynamics, quantum electrodynamics and other field models," 2014. Proceedings of Science, PoS (Baldin ISHEPP XXII) 027 http://pos.sissa.it/archive/conferences/225/027/Baldin ISHEPP XXII_027.pdf.

[7] K. Varga and Y. Suzuki, "Solution of few-body problems with the stochastic variational method. I. Central forces with zero orbital momentum," *Comp. Phys. Comm.*, vol. **106**, p. 157, 1997.

[8] K. Varga and Y. Suzuki, "Precise solution of few-body problems with the stochastic variational method on a correlated Gaussian basis," *Phys. Rev. C*, vol. **52**, p. 2885, 1995.

[9] Y. Suzuki and K. Varga, *Stochastic variational approach to quantum-mechanical few-body problems*. Berlin, Heidelberg: Springer-Verlag, 1998.

[10] J. R. Taylor, *Scattering Theory: The quantum theory of nonrelativistic collisions*. New York: Dover, 2006.

[11] M. L. Goldberger and K. M. Watson, *Collision theory*. New York: J. Wiley & Sons, 1964.

[12] K. A. Olive et al. (Particle Data Group), "Review of particle physics," *Chin. Phys. C*, vol. **38**, p. 090001, 2014. http://pdg.lbl.gov/xsect/contents.html.

[13] G. Audi and A. H. Wapstra, "The 1993 atomic mass evaluation. (I) Atomic mass table," *Nucl. Phys. A*, vol. **565**, p. 1, 1993.

[14] C. Samanta, P. R. Chowdhury, and D. N. Basu, "Generalized mass formula for non-strange and hyper nuclei with SU(6) symmetry breaking," *J. Phys. G*, vol. **32**, p. 363, 2006. arXiv:nucl-th/0504085.

[15] J. Cudell, A. Lengyel, and E. Martynov, "The soft and hard Pomerons in hadron elastic scattering at small t," *Phys. Rev. D*, vol. **73**, p. 034008, 2006. arXiv:hep-ph/0511073; http://www.theo.phys.ulg.ac.be/˜cudell/data/.